

**RS-8232-2/70220**

*Cy 2*

# SANDIA REPORT

SAND89-8732  
Unlimited Release  
Printed April 1990

## The Embrittlement of U-0.8% Ti By Absorbed Hydrogen

(To be published in Proceedings of 4th International Conference on Hydrogen Effects on Material Behavior, Jackson Lake Lodge, WY, September 1990)



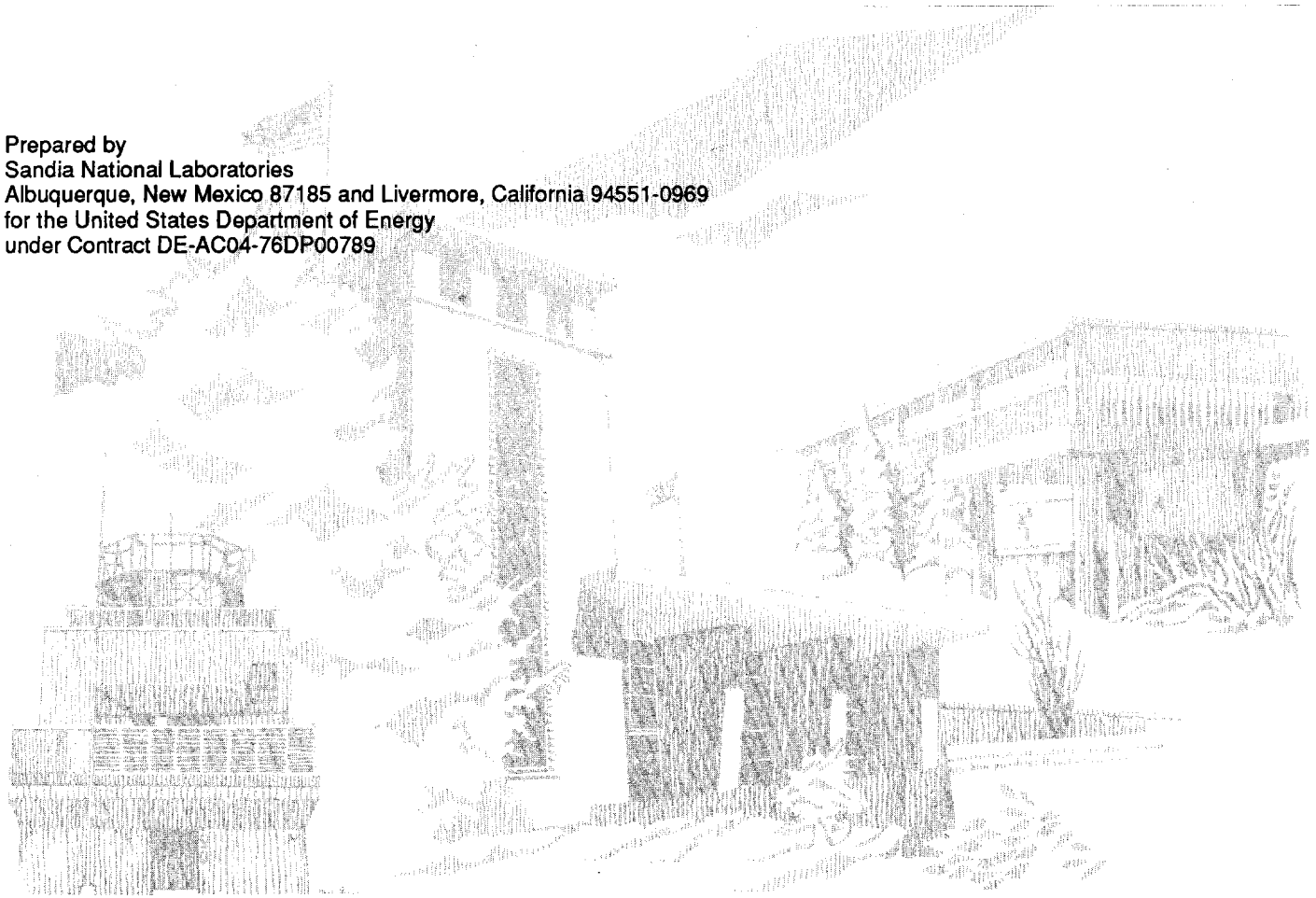
8232-2//070220

B. C. Odegard Jr, K. H. Eckelmeyer, and J. J. Dillon



00030002 -

Prepared by  
Sandia National Laboratories  
Albuquerque, New Mexico 87185 and Livermore, California 94551-0969  
for the United States Department of Energy  
under Contract DE-AC04-76DP00789



Issued by Sandia National Laboratories, operated for the United States Department of Energy by Sandia Corporation.

**NOTICE:** This report was prepared as an account of work sponsored by an agency of the United States Government. Neither the United States Government nor any agency thereof, nor any of their employees, nor any of the contractors, subcontractors, or their employees, makes any warranty, express or implied, or assumes any legal liability or responsibility for the accuracy, completeness, or usefulness of any information, apparatus, product, or process disclosed, or represents that its use would not infringe privately owned rights. Reference herein to any specific commercial product, process, or service by trade name, trademark, manufacturer, or otherwise, does not necessarily constitute or imply its endorsement, recommendation, or favoring by the United States Government, any agency thereof or any of their contractors or subcontractors. The views and opinions expressed herein do not necessarily state or reflect those of the United States Government, any agency thereof or any of their contractors or subcontractors.

SAND89-8732  
Unlimited Release  
Printed April 1990

## THE EMBRITTLEMENT OF U-0.8%TI BY ABSORBED HYDROGEN

B. C. Odegard Jr\*, K.H. Eckelmeyer\*\*, and J. J. Dillon\*\*\*

\* Sandia National Laboratories, Livermore, CA

\*\* Sandia National Laboratories, Albuquerque, NM

\*\*\* Oak Ridge Y-12 Plant, Martin Marietta Energy Systems,  
Oak Ridge TN

### ABSTRACT

U-0.8%Ti is typically quenched from 800°C to produce an alpha phase martensite, and then aged at 350 to 400°C to obtain yield strengths of 750 to 1050 MPa. In the normal course of processing, residual hydrogen is introduced into the alloy which can affect the mechanical properties. This study will address the effects of relatively small hydrogen concentrations (<1.0 wppm) on the ductility and fracture behavior of this alloy.

In this study, smooth bar tensile specimens containing 0.06, 0.16, and 1.14 wppm hydrogen were tested in vacuum or dry argon at strain rates varying from  $10^{-6}$  to  $10^0$  s<sup>-1</sup> and temperatures varying from -35° to 110°C. The transition strain rate for hydrogen embrittlement as measured by the ductility parameters increased with increasing hydrogen and decreasing temperature. Correspondingly, the fracture process changed from transgranular dimple rupture to interfacial separation along martensitic plate boundaries. Evidence is presented to show that the fracture mechanism is due to hydride formation at the martensitic plate boundaries. Hydride formation is enhanced by an increase in hydrogen content, intermediate temperatures and a high triaxial stress state.

## Acknowledgments

The authors wish to thank the staff at the Sandia National Laboratories (Livermore, CA, and Albuquerque, NM) and the Y-12 Plant (Oak Ridge, TN) who have contributed to this study. A special thanks to P. W. Hatch (SNL), T. J. McCabe (SNL), and D. Zanini (SNL) for the mechanical testing; B. G. Brown (SNL) and D. H. Huskisson (SNL) for the SEM work; M. E. McAllaster (SNL) and A. Kilgo (SNL) for metallography; and G. L. Powell (Y-12) for hydrogen analysis. Also, a special thanks to messieurs E. L. Bird (Y-12), G. L. Powell (Y-12), H. R. Johnson (SNL), M. B. Loll (SNL), A. W. Thompson (Carnegie-Melon University) and madame B. A. Lomax (Y-12) for many useful discussions.

## Introduction

Uranium is used in a variety of applications because of its high density and special nuclear properties. Engineering requirements for moderate to high strength structural materials having densities in excess of  $18 \text{ g/cm}^3$  have led to the development of several simple binary uranium alloys. The alloy of this investigation, U-0.8%Ti, is processed by quenching from the gamma-field (BCC),  $>800^\circ\text{C}$ , to produce a supersaturated martensitic variant of the alpha-phase (orthorhombic) termed alpha prime. The alloy is then aged in the  $350\text{-}400^\circ\text{C}$  range to obtain the desired properties. During the period of strengthening, no change in the martensitic structure can be detected by metallographic examination. Transmission electron microscopy confirms that strengthening results from the formation of a fine, discrete precipitate,  $\text{U}_2\text{Ti}$ . Additional aging promotes the decomposition of the martensite to a fine composite of the equilibrium alpha and delta phases. A comprehensive study on the aging characteristics and microstructure of the U-0.8%Ti alloy has been published by Eckelmeyer and Zanner (1). The U-0.8%Ti is among the strongest of the dilute uranium alloys and can be aged to yield strengths of 750-1050 MPa.

### Hydrogen Effects in Alpha Uranium

Several investigations have discussed the influence of hydrogen on the properties of alpha uranium (2-8). That work suggests a mechanism for hydrogen embrittlement that is associated with the formation of a grain boundary hydride at very low hydrogen concentrations. For example, Davis (2), in an early study, noted that embrittlement occurs in alpha uranium at hydrogen concentrations greater than 0.4 wppm due to a grain boundary hydride. Gardner and Riches (3) later reported observing the presence of a grain boundary hydride at hydrogen concentrations of 0.12 wppm but noted that as the hydrogen concentration increased, the hydride became more discrete and widely distributed. They concluded that the degree of embrittlement was a function of the size of the hydride and that maximum embrittlement occurs at approximately 2.5 wppm hydrogen. Beevers and Newman (4), Owens (5), and Cotterill (6) in considering the evidence resulting from tests on alpha uranium, supported the grain boundary hydride theory. Inouye and Schaffhauser (7) studied the uptake of hydrogen as a function of pressure and temperature and concluded that at ambient conditions, virtually all of the hydrogen in alpha uranium is present as  $\text{UH}_3$ . Their study concluded that the ductility of uranium was drastically reduced when the hydrogen content exceeded approximately 0.2 wppm.

The effect of hydrogen-producing environments on the properties of alpha uranium was discussed by Adamson et al (8); whereby, they explained the similarities between internal hydrogen embrittlement and hydrogen generated by the reaction of water with uranium during static and dynamic tensile tests. Their studies concluded that the ductility parameters were reduced by both internal and environmental hydrogen. The fracture was intergranular and increasing the test temperature above  $100^\circ\text{C}$  eliminated the embrittlement. These observations were in agreement with the hydride embrittlement theory.

### Hydrogen Effects in U-0.8%Ti Alloy

The effects of hydrogen on the mechanical properties of U-0.8%Ti are similar to those in unalloyed alpha-uranium (9); Powell (9) notes these similarities in a study of hydrogen effects in uranium alloys. In his study, tensile properties were compared for material in the aged and unaged condition with varying hydrogen contents. The ductility was severely reduced by hydrogen concentrations less than 0.1 wppm in both conditions. In another paper by Powell (10), smooth bar tensile tests were conducted on aged U-0.8%Ti. He observed that at low hydrogen concentrations ( $<0.1$  wppm) and a strain rate of  $10^{-3}\text{sec}^{-1}$ , the fracture was primarily by microvoid coalescence with some evidence of fracture along martensitic plate boundaries. At

high hydrogen concentrations ( $>1$  wppm) with the same strain rate, the fracture occurred exclusively by interfacial separation along the martensitic plate boundaries. At high strain rates, less reduction in ductility was observed.

The influence of hydrogen-producing environments was demonstrated in the U-0.8%Ti alloy by Johnson et al (11). Smooth bar tensile tests exhibited noticeable reductions in the ductility parameters when tested in humid air. Verification of the deleterious effects of water vapor on the ductility of U-0.8%Ti is reported by Hemperly (12) in a study evaluating the use of rust inhibiting oils in protecting tensile bars during tests in high humidity environments.

### Objective

It is the purpose of this paper to evaluate the influence of hydrogen concentration, temperature, and strain rates upon the hydrogen embrittlement behavior of the U-0.8%Ti alloy. In discussing the hydrogen embrittlement of the U-0.8%Ti alloy, only the internal hydrogen effects will be addressed. Hydrogen-producing environments such as water vapor resulting from tests in ambient air, have been negated by testing only in dry air ( $<10\%$  RH) or vacuum.

## Experimental Procedure

The material in this study was processed to obtain hydrogen concentrations of 0.06, 0.16, and 1.14 wppm. The composition was  $0.8 \pm 0.05\%$  Ti (by weight), 1.14 wppm hydrogen (maximum), and trace amounts of carbon, iron, silicon, oxygen, and nitrogen. None of the trace elements exceeded 200 wppm. Hydrogen charging was easily accomplished during exposure to a salt bath furnace at  $630^\circ\text{C}$ . Water vapor in the environment reacts with the molten potassium carbonate salt to form hydroxyl ions. The reaction of the uranium with the hydroxyl ions produces uranium oxide and a high hydrogen activity that charges the alloy with hydrogen. The material blank exhibiting 1.14 wppm hydrogen was charged in the salt bath furnace for two hours, solutionized in argon at  $800^\circ\text{C}$ , and water quenched. The material blanks exhibiting the lower hydrogen concentrations (0.06, 0.16 wppm) were charged in the salt bath furnace for two hours, solutionized in a vacuum furnace at  $800^\circ\text{C}$ , and water quenched. The time in vacuum dictates the hydrogen concentration levels. The hydrogen concentration was determined using a quadrupole mass-spectrometry technique (13). Several analysis were taken from each blank to verify the hydrogen uniformity. The material blanks were then aged at  $385^\circ\text{C}$  for 4.5 hours in argon. This aging schedule produced material which exhibited a yield strength (0.2% offset) of approximately 965 MPa. The grain morphology in the gamma-quenched condition is similar to the martensite plate morphology seen in steels.

Smooth bar tensile specimens meeting the geometric requirements specified in ASTM E-8 were machined from the three heats of material. The specimens were then covered with a film of oil to prevent oxidation until the tests were conducted. In each case, the coating was removed prior to testing. The specimens were tested to failure using continuous extension at strain rates varying from  $10^{-6}$  to  $10^0$   $\text{s}^{-1}$  in increments of  $10^1$   $\text{s}^{-1}$  at several temperatures including:  $-35^\circ$ ,  $0^\circ$ ,  $20^\circ$ ,  $65^\circ$ , and  $110^\circ\text{C}$ . All tests were conducted either in vacuum or dry air ( $<10\%$  RH) to exclude external hydrogen embrittlement due to atmospheric water vapor.

Several smooth bar tensile specimens were subjected to a discontinuous loading mode to determine the influence of plastic flow on the embrittlement mechanism. Tensile specimens having a hydrogen concentration of 0.16 wppm were prestrained at strain levels of 1, 3, and 6% at a low strain rate ( $10^{-5}$   $\text{s}^{-1}$ ) followed by a high strain rate to failure ( $10^{-1}$   $\text{s}^{-1}$ ). Two

additional bars were prestrained to 3% at a strain rate of  $10^{-5} \text{ sec}^{-1}$ , held under load for 4 hours, and tested to failure at  $10^{-1} \text{ sec}^{-1}$ .

All broken specimens were subjected to fractographic analysis using a scanning electron microscope.

## Results and Discussion

The results of the room temperature tensile tests (continuous) with hydrogen concentrations of 0.06, 0.16, and 1.14 wppm are shown in Figure 1. The material exhibited a transition from ductile to brittle behavior at a strain rate of approximately  $10^{-3} \text{ s}^{-1}$ . This type of behavior is associated with a diffusion-controlled mechanism. That is, at the lower strain rates, sufficient time was available for hydrogen diffusion to the martensitic plate boundaries. In contrast, at the higher strain rates, insufficient time was available for hydrogen transport and thus a ductile fracture ensued. Below a strain rate of approximately  $10^{-3} \text{ s}^{-1}$ , the percent reduction in area (% RA) was less than 10% and the fracture mode was by interfacial separation along martensitic plate boundaries suggesting hydrogen diffusion to the plate boundaries and subsequent hydride formation. At the higher strain rates, the ductility was high and the fracture mode was transgranular, microvoid coalescence indicating insufficient time for the hydrogen concentration to reach a critical level for hydride formation at the plate boundaries. The critical strain rate for hydrogen embrittlement was influenced by hydrogen content as noted in Figure 1. The critical strain rate for embrittlement was increased slightly when the hydrogen content was increased from 0.06 to 0.16 wppm. This behavior suggests that, as the bulk hydrogen concentration increased, the diffusion distance necessary to reach a critical hydrogen concentration at the plate boundaries was decreased. When the hydrogen concentration was increased to 1.14 wppm, the ductility is consistently low regardless of the strain rate. This behavior suggests that the critical hydrogen concentration for hydride formation was present at the plate boundaries prior to testing. The micrographs in Figure 2 contrast the fracture mode in the room temperature tests for the specimens with a hydrogen content of 0.16 wppm at low and high strain rates. The fracture mode exhibited by the specimens charged to a 1.14 wppm hydrogen content is shown in Figure 3 for a strain rate of  $10^0 \text{ s}^{-1}$ . The fracture mode was independent of strain rate at this hydrogen concentration. The strength parameters were unaffected by the hydrogen concentrations.

The results of the pre-strained (discontinuous), room temperature tensile tests are shown in Table I. First, it is clear that except for two test bars, the prestrain in the uniform strain region did not influence the ductility parameters or the failure mode, thus dispelling the notion that dislocations were transporting hydrogen to the boundaries during plastic flow in the uniaxial strain region. Secondly, the presence of an inclusion, such as existed in the two ductility outliers, can promote a brittle fracture. That is, in the presence of a triaxial stress, generated by a large inclusion cluster or at the onset of necking as in the case of the continuous extension tensile tests, a brittle fracture was promoted. The effect of a sustained load was inconsequential to the embrittlement mechanism. The influence of a triaxial stress state on hydride forming materials is discussed below.

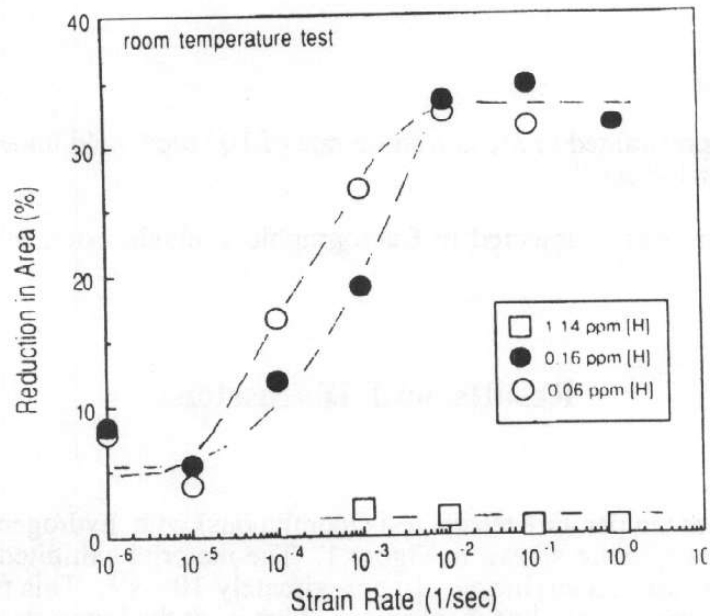


Figure 1. Percent reduction in area as a function of hydrogen content and strain rate. The test temperature was 20°C.

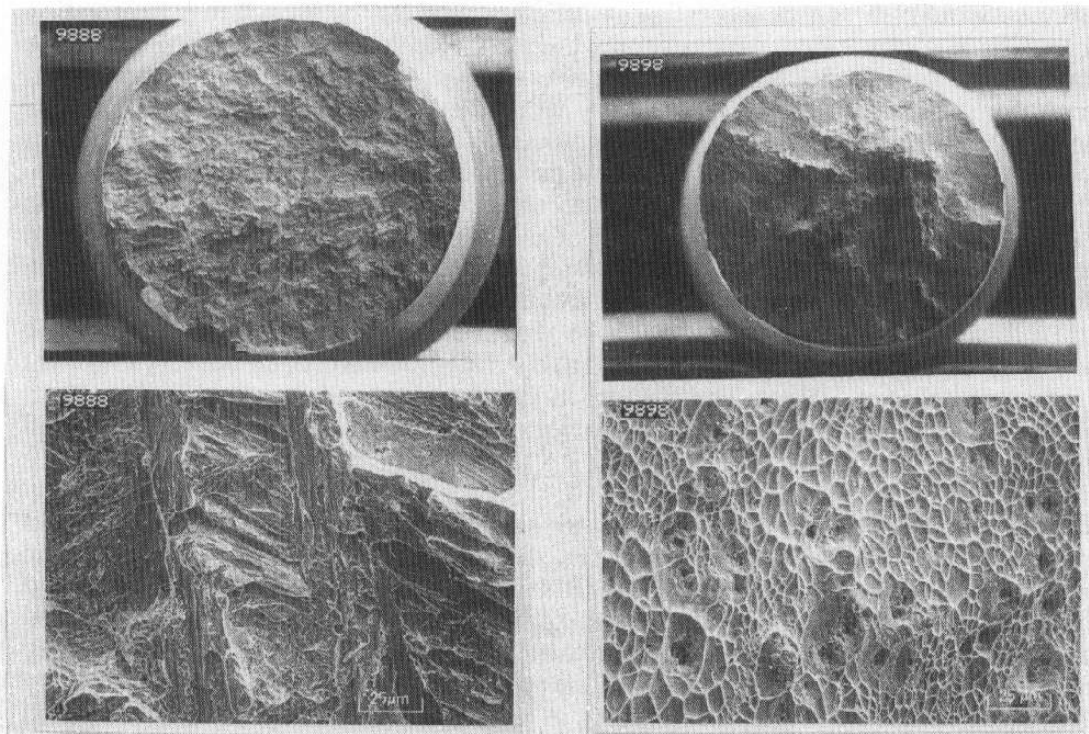


Figure 2 SEM showing fracture morphology on specimens tested at room temperature, (2a) low strain rate and (2b) high strain rate.

Sufficient experimental work on hydride-forming metals has shown that if the hydrogen concentration level is below some critical value (equilibrium hydrogen solvus), embrittlement

will not occur (14). However, under certain circumstances, local concentrations might rise above this level. This can occur under conditions of high triaxiality, such as at a crack-tip or an inclusion cluster. In a paper by Paton (14), two conditions for embrittlement by hydride formation in titanium alloys are discussed. The first is the effect of stress on the equilibrium hydrogen solvus, and the second is the effect of misfit on terminal solid solubility. Both would affect the propensity for hydride formation. In his paper, the hydrogen concentration in the presence of a hydrostatic stress is expressed as

$$C_H = C_H^0 \exp \left[ \frac{PV_H}{RT} \right] \quad (1)$$

where  $C_H^0$  is the solubility under zero stress, P is the hydrostatic component of the stress,  $V_H$  is the volume increase due to the hydrogen in solution, and R and T have their usual meaning. For the case of a hydrostatic tensile stress, the concentration of hydrogen will increase; and for a hydrostatic compressive stress the concentration will decrease. Therefore it is argued that there will be a hydrogen flux towards a stress concentrator such as an inclusion or crack-tip.

Table I. This data shows the effect of pre-straining at a low strain rate on the reduction in area of tensile bars with a hydrogen content of 0.16 wppm. The test temperature was 20°C.

Pre-Strain ( $10^{-5} \text{ s}^{-1}$ )	Test Rate	RA	Fracture Mode
1%	$10^{-1} \text{ sec}^{-1}$	37.3%	MVC
"	"	15.5%**	I/MVC
3%	"	35.8%	MVC
"	"	39.7%	MVC
6%	"	33.3%	MVC
"	"	32.4%	MVC
3%*	"	35.8%	MVC
3%*	"	4.9%**	I/MVC

\* Test bar was held under load at 3% strain for 4 hours prior to testing to failure.

\*\* Large inclusion cluster was fracture origin.

MVC Transgranular, microvoid coalescence

I Interfacial Separation

This concentration will be dependent on distance from the crack-tip and on the time and temperature after the application of the load. Concentrations of the order of 2-3 times the bulk material can easily be obtained after short periods of time under load. Thus, at an inclusion cluster, where the hydrostatic stress could be approximately three times the static yield stress, the hydrogen concentration could be greater than 1 wppm, which, as evidenced by the tests conducted on the U-0.8%Ti alloy with a hydrogen content of 1.14 wppm, would exhibit a brittle fracture. Whereas, in the absence of a stress gradient such as under the plane stress conditions existing in a tensile test prior to instability, the ratio,  $C_H/C_H^0$  is approximately equal to one (15) and embrittlement due to excess hydrogen is not expected.

The data generated in this study (Table I) suggest that a similar mechanism exists for the U-0.8%Ti alloy. In the smooth bar (discontinuous) tensile tests, slow strain rate loading in the uniform strain region did not produce a decrease in ductility when subsequently strained to failure at a high strain rate (Figure 4a). The fracture mode was transgranular microvoid coalescence. The data suggest that the strain-induced hydrogen concentration necessary for hydride formation at the martensitic plate boundaries was not promoted in the uniform strain region. However, in the presence of an inclusion, the stress-enhanced hydrogen concentration was sufficiently high to promote a brittle behavior at strain values as low as 1% (Table I). The fracture mode in this specimen was mixed with interfacial separation at the martensitic plate boundaries near the inclusion and microvoid coalescence at the shear lips (Figure 4b).

The effect of temperature on the observed hydrogen embrittlement in the U-0.8%Ti alloy is illustrated in Figure 5. A decrease in temperature increased the transition strain rate from  $3 \times 10^{-4} \text{ s}^{-1}$  at  $110^\circ\text{C}$  to approximately  $2 \times 10^{-2} \text{ s}^{-1}$  at  $0^\circ\text{C}$ , thus promoting a brittle fracture. An Arrhenius plot of this shift in the transition strain rate as a function of temperature gave a negative activation energy. This is consistent with hydride embrittlement in other alloys. Boyer and Spurr (16) showed that the maximum crack growth rate in titanium alloys was at an intermediate temperature. The crack growth rates were lower at the temperature extremes. The occurrence of this behavior can be described in terms of precipitation behavior(17). That is, the rate of

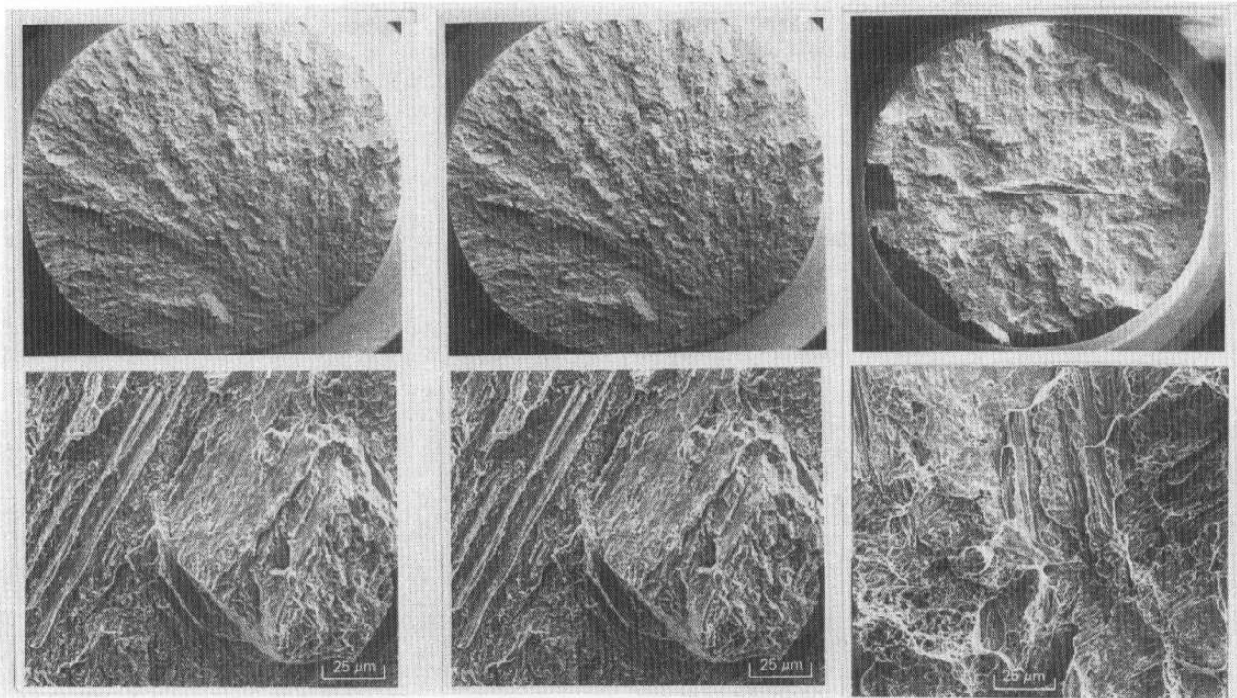


Figure 3. SEM showing fracture morphology on specimen having a 1.14 wppm hydrogen concentration. The strain rate was  $10^0 \text{ s}^{-1}$ .

4a  
4b  
Figure 4. SEM showing fracture morphology on specimens prestrained 3% (4a) and 1% (4b) indicating the influence of an inclusion on the fracture mode.

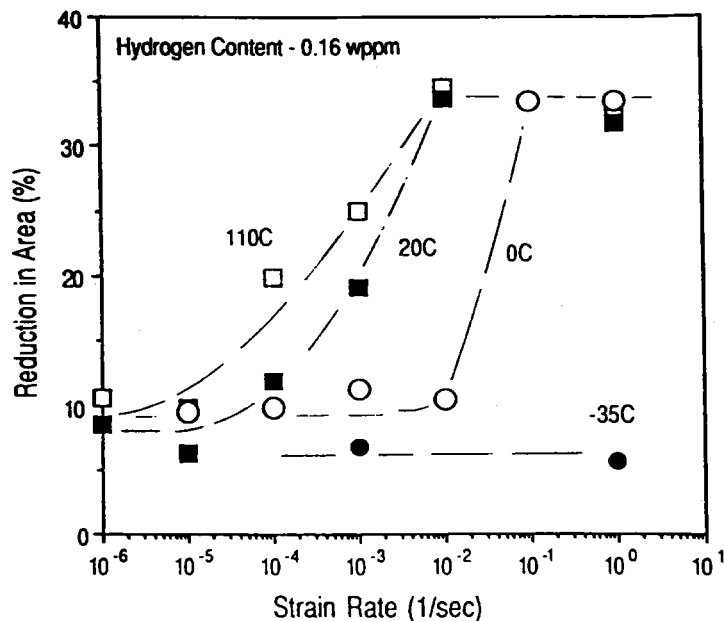


Figure 5. The percent reduction in area as a function of test temperature and strain rate. The hydrogen concentration is 0.16 wppm.

precipitation is decreased at high temperatures because the driving force is decreased as the solubility of the solute is increased. The rate of precipitation is decreased at low temperatures because the kinetics for the reaction are decreased. At 110°C, the fracture mode at the high strain rate was transgranular microvoid coalescence. At the low strain rates the fracture mode was interfacial separation. However, there were shallow microvoids forming along the martensitic plate boundaries indicative of a more ductile fracture at the higher temperature. At -35°C, the ductility was low and the fracture mode was interfacial separation along martensitic plate boundaries for all strain rates. The comparisons in fracture morphology are shown in Figures 6 and 7. This shift to a more brittle behavior rather than a more ductile behavior as noted in the titanium alloys is due to a brittle-to-ductile transition behavior. In unalloyed uranium there is a brittle-to-ductile transition at approximately room temperature. The factors affecting this temperature dependence are discussed in detail in references 5, 6. The U-0.8%Ti alloy exhibits a brittle to ductile transition temperature (BDTT) at approximately -30°C (11). The net result is that the embrittlement of the U-0.8%Ti alloy by the hydride is decreased at higher temperatures. At low temperatures (i.e., below the BDTT), the effect of the transition in deformation modes (5) promotes a brittle fracture regardless of the hydrogen content. The fracture mode of the tensile bars tested at -35°C were similar to the fractures promoted by hydride embrittlement.

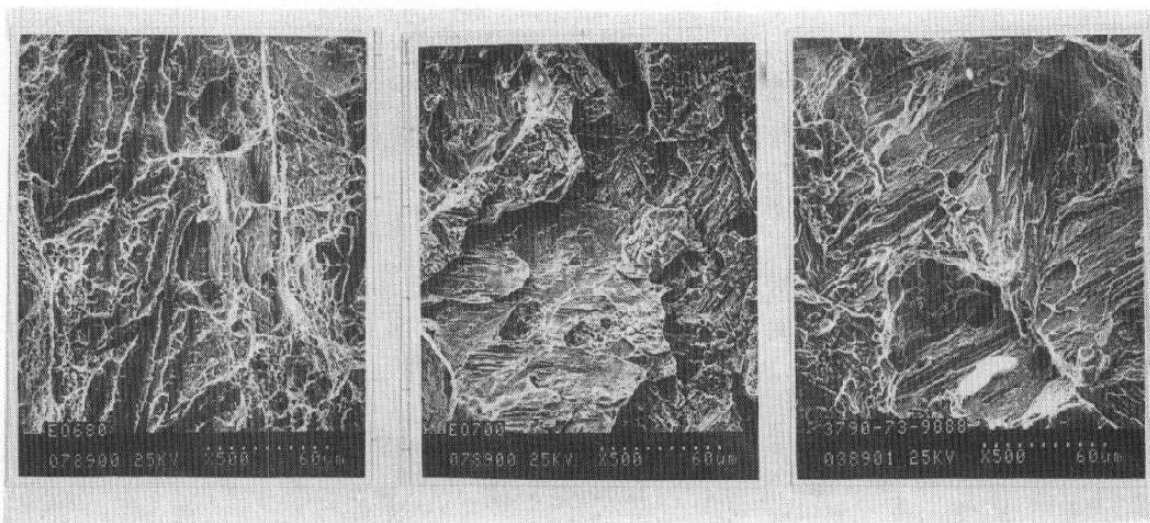


Figure 6. SEM showing the fracture morphology on specimens tested at 110° (a), 20° (b), -35°C (c) at a strain rate of  $10^{-6} \text{ sec}^{-1}$ .

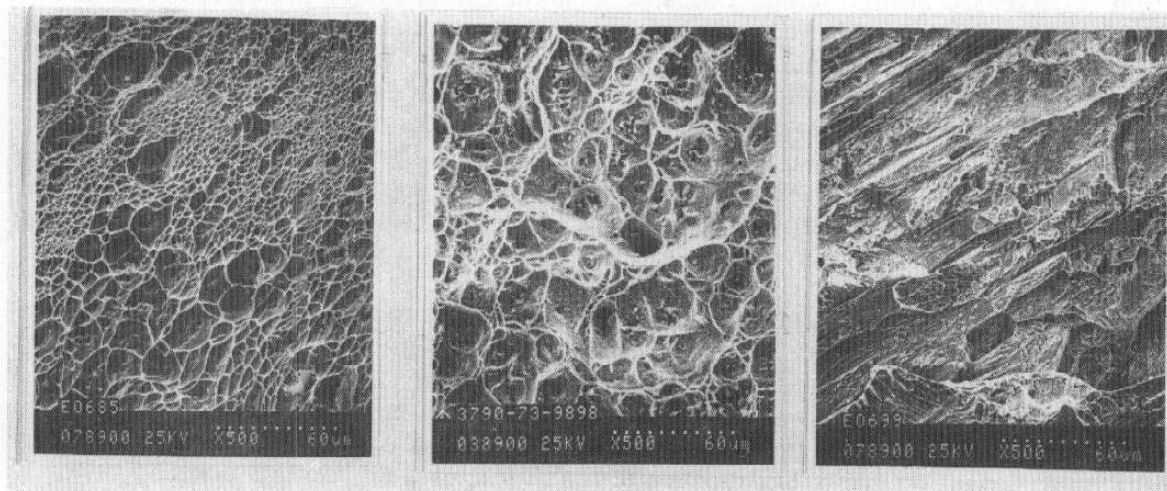


Figure 7. SEM showing the fracture morphology on specimens tested at 110° (a), 20° (b), and -35°C (c) at a strain rate of  $10^0 \text{ sec}^{-1}$ .

## Conclusions

1. The U-0.8%Ti alloy is embrittled by the formation of uranium hydride at the martensitic plate boundaries. Hydrogen concentrations as low as 0.06 wppm were sufficient to promote brittle fracture at low strain rates.
2. The transition strain rate for hydrogen embrittlement is increased as the hydrogen content is increased. At sufficiently high hydrogen contents the material was brittle at all strain rates due to the presence of uranium hydride along the martensitic plate boundaries.
3. The transition strain rate for hydrogen embrittlement, in the temperature range  $-35^{\circ}\text{C}$  to  $110^{\circ}\text{C}$ , is decreased as the temperature is increased. However, at  $-35^{\circ}\text{C}$  the degree of embrittlement is superceded by the influence of a BDTT phenomenon.
4. Strain-induced precipitation of hydrides occurs in the presence of a triaxial stress state generated following the onset of necking or by a large inclusion. Plastic flow in the uniaxial strain region does not promote hydride formation and subsequent brittle fracture.

## References

1. K. H. Eckelmeyer and F. J. Zanner: *Journal of Nuclear Materials* , 1976, Vol. 62, pp. 37-49.
2. W. D. Davis: "Solubility, Determination, Diffusion and Mechanical Effects of Hydrogen in Uranium," Knowles Atomic Power Laboratory, Schenectady, N.Y. USAEC Contract Report Number KAPL-1548, August 1956.
3. H. R. Gardner and J. W. Riches: *Trans A.S.M.*, 1958, Vol. 50, pp. 729-747.
4. C. J. Beevers and G.T. Newman: *Journal of Nuclear Materials* , 1967, Vol. 23, pp. 10-18.
5. W. L. Owens: *Metallurgia*, 1962, Vol. 66, pp. 3-6.
6. P. Cotterill: "The Hydrogen Embrittlement of Metals," *Progress in Material Science*, 1961, Vol. 9, pp. 205-301.
7. H. Inouye and A. C. Schaffhauser: "Low-Temperature Ductility and Hydrogen Embrittlement of Uranium - A Literature Review," Oak Ridge National Laboratory, Oak Ridge, TN, USAEC Contract Report Number ORNL -TM-2563.
8. P. Adamson, S. Orman and G. J. Picton: *Journal of Nuclear Materials*, 1969, vol. 33, pp. 215-224.
9. G. L. Powell and J. B. Condon: "Hydrogen in Uranium Alloys," *Proceedings of the Conference on the Physical Metallurgy of Uranium Alloys*, Army Materials and Mechanics Research Center, Vail, CO, 1974.
10. G. L. Powell : "Internal Hydrogen in Uranium Alloys," *Proceedings of the Conference on the Metallurgical technology of Uranium and Uranium Alloys*, American Society of Metals, Gatinsburg, TN, 1981.
11. H. R. Johnson, J. W. Dini and S. W. Zehr: "On the Embrittlement of Uranium and U-0.8%Ti Alloy by Hydrogen and Water," *Proceeding of the Conference on Hydrogen in Metals*, American Society of Metals, Seven Springs, Champion, PA, 1973, pp. 325-344.
12. V. C. Hemperly: "Effect of the Relative Humidity in Test Atmospheres on U-0.75%Ti and U-2.25%Nb Alloys," Oak Ridge Y-12 Plant, Oak Ridge, TN, Report Number 20.
13. G.L. Powell, "A Method for Measuring the Hydrogen Content of Metals," *Proceedings of the Conference on Hydrogen in Metals*, American Society of Metals, Seven Springs, Champion, PA, 1973, pp. 585-593.
14. N. E. Paton: "Low Temperature Hydrogen Embrittlement of Titanium Alloys," *Proceedings of the Conference on Titanium, Science and Technology*, vol. IV, Munich, Germany, 1984, pp. 2519-2526.
15. W. W. Gerberich, T. Livne, X. F. Chen, and M. Kaczorowski: *Met. Trans.*, 1988, Vol. 19A, pp. 1319-1334.

16. R. R. Boyer and W. F. Spurr: *Met. Trans.*, 1978, Vol. 3, pp. 23-26.
17. N. E. Paton and J. C. Williams: "Effect of Hydrogen on Titanium and Its Alloys", *Proceedings of the Conference on Hydrogen in Metals*, American Society of Metals, Seven Springs, Champion, PA, 1973, pp. 409-431.

UNLIMITED RELEASE

INITIAL DISTRIBUTION

Y-12 Plant, Martin Marietta Energy Systems  
P.O. Box. 2009  
Oak Ridge, TN, 37831  
J. J. Dillon, 9202 MS 8096 (10)  
W. G. Northcutt Jr, 9202 MS 8096  
E. L. Bird, 9202 MS 8096  
B. A. Lomax, 9204-4 MS 8150  
L. G. Porter, 9113 MS 8202  
T. B. Conley, 9113 MS 8202  
L. E. Pender, 9723-11A MS 8127

D. H. Wood, LLNL, L355

1800 R. J. Eagan  
1810 D. W. Schaefer  
1820 J. B. Woodard  
1822 K. H. Eckelmeyer (10)  
1830 M. J. Davis  
1831 A. D. Romig

8000 J.C. Crawford  
attn: E. E. Ives, 8100  
R. J. Detry, 8200  
R. C. Wayne, 8400  
P. E. Brewer, 8500

8160 D. J. Bohrer  
attn: D. J. Beyer, 8163  
G. C. Story, 8165

8163 M. B. Loll  
8300 P. L. Mattern  
attn: W. Bauer, 8340  
W. J. McLean (acting), 8350  
W. J. McLean, 8360

8310 D. L. Lindner (acting)  
attn: D. L. Lindner, 8311  
M. I. Baskes, 8312  
J. M. Hruba, 8313  
M. W. Perra, 8314  
R. E. Stoltz, 8316

8312 B. C. Odegard, Jr, (10)

8535 Publications for OSTI (10)  
8535 Publications/Technical Library Processes, 3141  
3141 Technical Library Processes Division (3)  
8524-2 Central Technical Files (3)



8232-2/070220



00030002 -



8232-2/070220



00030002 -



8232-2/070220



00030002 -

